RESEARCH ARTICLE

JSFA Reports SCI

Casein-based nanocarriers for encapsulation of propolis extract: Design, fabrication, and characterization

Javad Feizy[1] | Mansooreh Soleimanifard[2] | Francesca Maestrelli[3] 🔾

[1]Department of Food Safety and Quality Control, Research Institute of Food Science and Technology (RIFST), Mashhad, Iran

[2]Department of Agricultural Sciences and Natural Resources, Ardakan University, Ardakan, Iran

[3]Department of Chemistry 'Ugo Schiff', University of Florence, Florence, Italy

Correspondence

Mansooreh Soleimanifard, Department of Agricultural Sciences and Natural Resources, Ardakan University, Ardakan, Iran.
Email: mansooresoleimani14@gmail.com

Maestrelli Francesca, Department of Chemistry 'Ugo Schiff', University of Florence, Florence, Italy.
Email: francesca.maestrelli@unifi.it

Abstract

Background: Propolis exhibits multiple biological and pharmacological properties attributed to the presence of natural bio active compounds. In spite of its potential healthy effects, its use in health-food and pharmaceutical products is very restricted due to its intense aroma, highly unstable, low aqueous solubility, and low bioavailability. The purpose of this study is to fabricate an appropriate, stable, and biodegradable casein-based nanocarrier as propolis delivery system. Propolis-loaded casein nanocarriers were prepared at different propolis extract/ caseinate ratio and assessed for physicochemical, structural, and thermal properties.

Results: The nanocarriers showed an increase of particle size augmenting propolis extract/ caseinate ratio and caseinate concentration. Image processing studies revealed an increase in L^* parameter (89.743), while b^* parameter revealed a reduction in the yellow color (14.655) increasing the amount propolis extract in the nanocarrier. Surface photomicrographs evidenced that an increment of propolis extract decreased the network compactness of the nanocarriers correlated with the lower entrapment of propolis extract into carriers at higher propolis extract/caseinate ratio. X-ray diffraction pattern suggested that propolis encapsulation produced a decrement in the caseinate crystallinity while differential scanning calorimetry and thermogravimetric/differential thermal analysis thermograms evidenced an increment of thermal stability of nanocarrier with increasing propolis extract content.

Conclusion: Propolis extract encapsulated within casein nanocarriers represented convenient physicochemical attributes and could provide as bioactive load in food/medical system.

KEYWORDS
casein nanocarriers, encapsulation, propolis extract, protein-based delivery system

INTRODUCTION

Propolis or bee glue is a natural resinous mixture, that honey bees produce by mixing saliva and beeswax with exudate from plants.[1,2] Propolis is one of the richest sources of bioactive compound and possesses numerous biological activities such as antimicrobial, anti-inflammatory, antiulcer, hepatoprotective, antitumor, immunostimulant, and antioxidant.[3] Notwithstanding significant promise of propolis as a bioactive composition, its health-food/pharmaceutical applicability is reduced due to its strong aroma, low aqueous solubility, and low

bioavailability.[4–6] Over the decades, the encapsulation strategy has utilized as emerging multi-disciplinarian platform, to shield the bioactive ingredients to overcome environmental stresses (the instability of ingredients during processing, storage, distribution, and physicochemical interactions)[7] as well as to improve bioavailability, taste, texture, and consistency of food products or mask an unpleasant feature such as strong aroma, and resinous behavior.[8,9] Nowadays, a significant trend for utilization of food-grade biopolymers as matrix in nanoscaled delivery systems has expanded dramatically to ameliorate well-being and human health.[10,11] Milk proteins, in particular casein, exhibit

multifunctional properties (biodegradability, biocompatibility) and can be applied for the formulation of nanoparticles for the protection and delivery of bioactive ingredients.[12] These carriers are able to self-assemble without the need for emulsifiers and stabilizers and can be easily prepared showing versatile applications changing pH, temperature, ionic strength, and solvent conditions. Moreover casein has good digestibility and stability, is safe, and can protect and control the release of the entrapped ingredients in the gastrointestinal tract.[11–15] Caseinates are obtained via acid sedimentation of native caseins from bovine milk at the isoelectric point, and sodium caseinate (NaCas) are afterward procured by neutralization and drying process of precipitated protein.[16] As an aqueous-soluble biopolymer with randomly coiled structure and unique self-binding character, NaCas hosts both hydrophobic and hydrophilic molecules, making it a valid carrier to encapsulate an extensive variety of bioactive agents.[7,17,18] NaCas is an attractive carrier that has been used for the delivery of poorly water soluble natural ingredients such as folic acid, quercetin, naringenin, curcumin, vitamin D, sesamol, curcumin, quercetin, and eugenol.[13,19–26] Recently, we successfully obtained sodium caseinate-maltodextrin nanocomplex nanocarriers loaded with propolis extract (PE).[27] In this context, the major purposes of this work were to design and optimize the preparation of nano-sized casein-based carriers to encapsulate PE. Dynamic light scattering (DLS), differential scanning calorimetry (DSC), thermogravimetric analysis (TGA), differential thermal analysis (DTA), field-emission scanning electron microscopy (FE-SEM), and image processing (L^*, a^*, b^*, C and $H°$) studies were performed to characterize such systems. Aim of the study is prepare stable of PE-NaCas nanoparticles and fill the gap of food applicability in harsh condition. Also, casein-based delivery systems containing PE can have potential applications to meliorate health and well-being.

MATERIALS AND METHODS

Materials

The raw propolis sample was purchased from local beekeepers (Khorramabad, Iran) in May 2019 and was stored at $-80°C$ until applied in the laboratory. Sodium caseinate (NaCas), tween-80, Folin–Ciocalteu phenol reagent, 2,2-diphenyl-1-picrylhydrazyl (DPPH) reagent were from Sigma-Aldrich (Germany/Switzerland/USA). Ethyl alcohol, calcium chloride, sodium hydroxide, hydrochloric acid, sodium carbonate, Folin–Ciocalteu reagent, gallic acid, and other chemicals/solvents were of the analytical grade and obtained from Sigma Aldrich (Saint Louis, MO, USA) or Merck (Darmstadt, Germany).

Preparation of PE

PE was prepared according to the method proposed by Silva et al., 2012, with some modification.[28] Briefly, 10 g of freeze-dried propolis, previously grinded in a ball mill (Marconi 350, Brazil), was placed in 100 mL of ethanol: water mixture (70:30 v/v) in an incubator shaker for 24 h (Quimis 255, Brazil) at $25°C$. The mixture was placed in an ultrasonic bath apparatus for 15 min, centrifuged (15,000 rpm, 10 min, $25°C$), and filtered using 0.45-μm cellulose filters. Finally, the filtrated was lyophilized (Liobras L101, Brazil) and kept at $-80°C$.

Preparation of casein nanocarriers

Formulation of PE-loaded nanocarriers (FP) and void carriers (FV) was performed by dissolving 1 or 2 g NaCas in 100 mL of distilled water adjusted to pH 7.0 (with 0.1 mol/L NaOH or HCl), under stirring for 30 min and let at $25°C$ overnight for hydration. Then, for FP formulation, PE was added at different concentrations (0.1, 0.2, 0. 4 and 0.8 g/100 mL) and homogenized (Ultra Turrax, IKA-T25, Germany) at 4000 rpm for 5 min. Thereafter, a $CaCl_2$ solution (2.0% w/v) as cross-linking agent was added under mild stirring for 2 h. Finally, resulting systems treated with the ultrasound bath (Powersonic 505, South Korea) at $40°C$ for 15 min. At the end of operation, the final supernatant was freeze-dried (Terroni, Brazil) and kept at $-80°C$ for further analyses. Void NaCas nanocarrier were prepared at 1% and 2% of NaCas and named FV1 and FV2, respectively. Loaded PE-NaCas nanocarriers were prepared at 1% of NaCas with a ratio of core material (PE) to protein (NaCas) of 1:10, 1:5, 1:2.5, and 1: 1.25 (w/w) (titration of system to pH = 4.1 with 0.1 N HCL) and called FP1, FP2, FP3, and FP4 respectively. Loaded PE-NaCas nanocarriers at 2% of NaCas was prepared with a ratio of core material (PE) to protein (NaCas) of 1:20, 1:10, 1:5, 1:2.5 (w/w) (titration of system to pH = 4.1 with 0.1 N HCL) and were named: FP5, FP6, FP7, and FP8.

Casein nanoparticles characterization

In order to calculate the amount of PE entrapped within casein nanocarrier (encapsulation efficiency, EE), the concentration of PE in the supernatants was determined by using the Folin–Ciocalteu method.[1,29] First, to plot a calibration curve about 0.5 mL of the diluted PE (1:50 v/v, at the concentration of 0.4 mg mL^{-1}) were mixed with 2.5 mL of 0.2 M Folin–Ciocalteu reagent and after 5 min, 2 mL of Na_2CO_3 solution (7.5%) was added. Absorbance reading of the mixture was carried out after 2 h incubation at room temperature at 725 nm using a spectrophotometer. Gallic acid was applied as a standard for calibration curve. The calibration curve was obtained using ready gallic acid standard solutions (5–500 mg/L) ($y = 0.014x + 0.0168$, $R^2 = 0.998$).

The concentration of total phenolic compounds (TPC) is expressed as the gallic acid equivalents (mg GAE/g) in dry weight.[28] To this purpose, 10 mg of nanocarriers was submerged in 10 mL of ethyl alcohol to wash the nonencapsulated phenolic compounds, then about 1 mL of the prepared sample was mixed with 10 mL hexane, sonicated (under shaking ~10 min), homogenized (~1 min at 12,000 rpm) and kept in a water bath (under stirring, ~24 h at $25°C$). During this operation, entrapped PE was released from the nanocarriers. Afterward, samples were centrifuged at 10,000 rpm for 15 min

at 25°C (EBA 270, Hettich centrifuge, Germany) and surnatant concentration was calculated using the calibration curve and TPC was measured by following Equation (1):

$$TPC\,(\%) = \frac{Measured\,PE\,in\,nanocarriers}{Initial\,PE\,added\,to\,the\,formulation}. \qquad (1)$$

The measurement of the total phenolic compound solid (TPCS) amount of outside of nanocarriers were performed measuring the non-encapsulated phenolic compounds in the ethyl alcohol solution passed through a syringe filter (0.45 nm) as described by Umesha et al.[30] with some modifications. The filtrate absorbance was estimated spectrophotometrically as described above and according to the Equation (2):

$$TPCS\,(\%) = \frac{Measured\,PE\,in\,filtrate}{Initial\,PE\,added\,to\,the\,formulation}. \qquad (2)$$

The EE of the PE-loaded nanocarriers was assessed using the following Equation (3):

$$EE\% = \frac{(TPC - TPCS)}{TPC} \times 100. \qquad (3)$$

In this equation, TPC represents total phenolic compounds of nanocarriers, inside or outside, and TPCS represents total phenolic compound solid on surface, that is, outside of nanocarriers.

The mean particle size, polydispersity index (PDI) and zeta potential of the nanocarriers was characterized by laser diffraction, using a Photon Correlation Spectroscopy (Zetasizer Nano SP90, Malvern, UK). In order to prepare stock solutions, about 10 mg of each nanocarrier was dispersed within 10 mL water, upon mild stirring at 50°C ∼ 1 h. The solutions were centrifuged at 15,000 rpm (∼15 min, 25°C) to expurgate the discarded matter, then the supernatant analyzed in triplicate at time 1 day after preparation at 25 ± 0.5°C. The yield of the nanocarriers was assessed pursuant to the solid content of the final nanocarriers, their constituents, and PE, according to Equation (4), as follow:

$$Process\,yield\,(\%) = \frac{(\,Weight\,of\,nanocarriers\,)}{(Weight\,of\,total\,solids\,within\,the\,formulation\,)} \times 100. \qquad (4)$$

Measurement of color

In order to peruse the effect of PE and encapsulation method on the color of casein-based nanocarriers, color indices (a^*, b^*, L^*) were appraised using a scanner apparatus (CanoScan LiDE220, Vietnam) with resolution of 300 DPI and color analysis was carried out using Image J software (http://imagej.net). In general, Using the Plugin tab, Color space converter section, Color conversion icon, the images were changed from RGB to LAB mode/format, and color indices (L^*, a^*, and b^*) were identified as a separate image. Finally, by activating the

software analysis section, the amount of L^*, a^*, and b^* were measured. The indices of chroma and Hue angle were computed using the following Equations (5 and 6) and the mean of three replicates were reported:

$$\left(\frac{b}{a}\right). \qquad (5)$$

$$Chroma = \left[(a)^2 + (b)^2\right]^{1/2}. \qquad (6)$$

Morphological analysis

The surfaces of the nanocarriers were appraised by FE-SEM (FE_SEM, TESCAN, Czech) according to the modified methodology described.[31] Before imaging, specimens were sputter-coated with gold palladium layer, and thus, FE-SEM was operated at acceleration voltage of 15 kV and working distance of 10 mm. Pictures were taken with different magnifications levels (1000× was reported as example).

X-ray diffraction analysis

In order to detect the crystalline or amorphous structure of the casein-based nanocarriers, their constituents and PE, x-ray diffraction (XRD) patterns were specified using an x-ray diffractometer (Bruker D-8 Advance, USA), under monochromatic radiation CuKα (1.5444 Âμm) operating at 40 kV/40 mA at an angular sweep 2θ ranging from 1 to 80° with intervals of 0.05° at each 1 s. The crystalline index was calculated using the following Equation (7):

$$Crystalline\,Index = \frac{crystalline\,area}{crystalline\,area + amorphous\,area} \times 100. \qquad (7)$$

Thermal properties

Differential scanning calorimetry

The nanocarries and their constituents were characterized by DSC (DSC 200 F3, Netzsch, Germany). About 5 mg of each of specimen was placed in an aluminum pan, then hermetically sealed. An empty pan was also utilized as the reference sample. The experiment was conducted in the 25–400°C temperature range at a constant heating rate of 10°C/min under a nitrogen flow of 50 mL/min.

TGA and DTA

The thermal stability of the casein-based nanocarriers investigated using TGA and DTA in a TA Instrument, model Q-500 (New Castle, DE, USA). The examinations were performed from the room temperature up to 400°C under nitrogen atmosphere at the constant heating rate of 10°C/min.

TABLE 1 Values of size- average, polydispersity index (PDI), zeta potential, and encapsulation efficiency (EE) of propolis extract (PE)-loaded nanocarriers.

Treatments	Ratio (PE: NaCas)	Size-average (nm)	PDI	Zeta potential (mV)	EE (%)	Yield (%)
FV1	(0:10)	328.1 ± 3.7j	0.49 ± 0.15e	−0.64 ± 0.08e	-	
FP1	(1: 10)	356.5 ± 2.5i	0.54 ± 0.07e	−6.30 ± 1.63d	87.34 ± 3.11b	78.2 ± 2.15b
FP2	(1: 5)	394.2 ± 4.7h	0.59 ± 0.12d	n.d.	80.53 ± 2.12c	76.4 ± 2.21c
FP3	(1: 2.5)	599.5 ± 3.6f	0.63 ± 0.10c	−18.60 ± 2.84a	74.64 ± 1.46d	74.1 ± 1.18d
FP4	(1:1.125)	1207.5 ± 5.1b	0.69 ± 0.14b	n.d.	63.41 ± 3.21e	71.7 ± 1.44e
FV2	(0:20)	510.7 ± 1.9g	0.55 ± 0.03e	−0.78 ± 0.04e	-	
FP5	(1:20)	698.5 ± 4.8e	0.71 ± 0.11c	n.d.	94.14 ± 2.42a	81.4 ± 3.25a
FP6	(1:10)	712.0 ± 3.1d	0.56 ± 0.14d	−15.1 ± 1.4b	88.16 ± 2.35b	79.8 ± 1.61b
FP7	(1: 5)	1092.2 ± 2.3c	0.65 ± 0.11b	−8.5 ± 2.4c	81.26 ± 4.18c	79.3 ± 2.74c
FP8	(1:2.5)	1501.0 ± 10.2a	0.73 ± 0.18a	n.d.	74.57 ± 2.37d	76.7 ± 1.36d

Note: Different lower-case letters indicate a significant difference at $p < 0.05$ in each column.

Statistical analysis

The acquired datum was represented as the mean along with standard deviation of triplicate designations (exclusive of FE-SEM, x-ray, DSC, TGA, and DTA results). To assess statistical significance among samples, analysis of variance ($p < 0.05$, 0.01) and the mean comparison were performed by one-way ANOVA approach using the SPSS 24 software (SPSS Inc., Chicago, IL, USA) at $p < 0.05$ and 0.01.

RESULTS AND DISCUSSION

Determination of phenolic content in raw propolis

Propolis has phenolic content of 74.9 mg/100 g.

Particle characterization

The results obtained, in terms of particle size, PDI, zeta potential, EE, and yield, are reported in Table 1. As shown nanocarriers depicted sizes between 356.5 ± 2.5 nm and 1501.0 ± 10.2 nm. The results reveal that, increasing concentration of casein, the particle size of the nanocarriers increase in accordance with previous results.[31] In fact, significant difference ($p < 0.05$) was appreciated between the two wall materials concentration groups (F1 vs. F2 group). Moreover, the analysis evidenced a positive relationship between PE and NaCas contents and particle size: in fact, void nanocarriers have the lower particle size and the size increases, increasing the PE content. This phenomenon was observed also by other authors that observed as propolis formulations are larger than void formulations which can agglomerate and increase the particle size due to aggregating smaller particles around larger ones.[32] In fact, also PDI increases, increasing PE amount. The values to zeta potential were between −18.6 to −10.1 mV showing a good stability for nanocarriers with code of FP1, FP3, FP6, and FP7, respectively, while it was not possible obtain valid

value for FP2, FP4, FP5, and FP8, as observed in a previous work.[27] At lower NaCas concentration (1%), increasing PE concentration, a negative charge rising was observed from −12.3 to −18.6 mV. In literature is reported that formulations with similar amount of protein showed an increase of negative charge, with rising PE concentration.[6,33] The values of EE ranged from 63.41 ± 3.21% (FP4) to 94.14 ± 2.42% (FP5) as epitomized in Table 1. An outstanding increment in EE% was apperceived decreasing the particle size, with the reduction in PE and increment casein concentrations, in fact the highest EE% was apperceived in FP5. Results in this study were consistent with results of other researchers.[31,34] As expected, the yield was superior for carriers with greater content of encapsulant (NaCas 2%) and a correlation was observed between PE/NaCas ratio and NaCas concentration and yield. Nanocarrier obtained with higher NaCas concentration with the lower PE (FP5) quantity exhibited the highest EE% and yield.

Color evaluation of casein-based nanocarriers

Color is one of the most important factors for quality and visual description of natural products. The color indices (a^*, b^*, L^*, $H°$, and C) for the powders are revealed in Table 2. In this technique, L^* indicates lightness on a 0–100 scale from black to white; a^*, (+) red and (−) green color ingredients; and b^*, (+) yellow and (−) blue color ingredients.[35] Changes in the color indices of the casein-based carriers were recorded when PE concentration and ratio of PE to NaCas changes. At lower NaCas content, it was realized that value of color parameters a^*, b^*, $H°$, and C increased with the increasing ratios of PE to NaCas used (FP1–FP4), while value of color parameter L^* decreased. This tendency can be associate with the intrinsic color of the PE which is yellow to brownish. In other hand, the PE–loaded casein-based nanocarriers produced at high level of NaCas demonstrated a superior L^* and $H°$ as well as lower a^*, b^*, and C compared with carriers produced at low level of NaCas, which was attributed to a better coverage of PE. The value of factor $H°$ is the description of color that is comprehended and all treatments (apart from FV1 and FV2) display values of

TABLE 2 Color properties of propolis extracted-loaded/void casein-based nanocarriers (mean ± SD, n = 3).

Treatments	L*	a*	b*	H (°)	C
FV1	73.611 ± 4.451f	2.012 ± 1.221a	5.176 ± 1.321 g	22.256 ± 2.613a	5.553 ± 1.241 g
FP1	87.210 ± 1.423b	−2.613 ± 0.234f	14.932 ± 2.113f	−9.99 ± 2.124f	15.158 ± 2.112f
FP2	87.099 ± 3.140b	−2.103 ± 0.452e	19.997 ± 6.154e	−5.970 ± 1.312d	20.107 ± 2.605d
FP3	86.301 ± 2.65b	−0.826 ± 1.240d	21.447 ± 2.165d	−2.057 ± 0.601c	21.462 ± 4.221d
FP4	80.462 ± 6.243e	0.607 ± 0.021c	25.77 ± 4.325b	−1.093 ± 0.521c	25.777 ± 4.125b
FV2	83.121 ± 1.213d	1.406 ± 0.158b	5.344 ± 0.561 g	15.052 ± 0.218b	5.347 ± 2.435 g
FP5	89.743 ± 7.150a	−2.567 ± 0.524f	14.655 ± 2.145f	−10.002 ± 2.157f	14.878 ± 2.135f
FP6	87.141 ± 2.255b	−2.369 ± 0.723f	19.462 ± 1.207e	−6.926 ± 1.348e	19.608 ± 4.204e
FP7	84.174 ± 2.157c	−2.021 ± 0.814e	22.943 ± 1.814c	−4.980 ± 0.417d	23.031 ± 2.314c
FP8	85.435 ± 4.124c	−2.051 ± 0.781e	27.237 ± 3.132a	−4.236 ± 3.154d	27.314 ± 7.641a

Note: (A) a* (redness-greenness); (B) b* (yellowness-blueness); (C) C* (chroma); (D) H° (Hue angle); and (E) L* (whiteness-blackness) of samples. Different lower-case letters indicate a significant difference at $p < 0.05$ in each column.

factor $H° < 10$, accordingly they can be depicted as red ($-a^* =$ green color) treatments.[35,36] The value of color parameter C was proportionate to the intensity of the color and represents its degree of saturation, this datum proposes efficacy of higher resistance of red color in carriers acquired.[37] According to Obón et al.[38] a pilgarlic color variance from 0 to 1.5 demonstrates that visually the treatment is approximately similar to the principal one, whereas in the 1.5 to 5 range, the discord in color can be discerned. In other research, encapsulated freeze-dried saffron petal's extract with various matrices such as gum Arabic and maltodextrin as well as announced, they observed that increase in the anthocyanins content led to an increment in a^* value, decrease in b^* value and L^*, as well as color of powders get darker after storage.[39] This demonstrate that the color indices were affected by process parameters such as well as method of encapsulation. Finally, it should be noted that casein-based nanocarriers displayed a light/intense yellow color visually that it was consistent with the results of factor $H°$.

Field-emission scanning electron microscopy

The photomicrographs of the void batches exhibited sponge-like matrices with regular shapes and some pores on the surface, as shown in Figure 1 (FV1 and FV2). A different morphology was observed for PE-loaded (FP4–FP8) carriers, showing spherical particles with regular shapes, homogeneous and smooth surface without any pores or cracks or interruptions, suggesting the homogeneous distribution of PE into casein-based nanocarriers and adaptability between core and wall materials. Also, the other photomicrographs of the PE-loaded casein-based nanocarriers showed similar results. Similar results were obtained by other authors applying the similar drying method.[29,31] It is remarkable that the concentration of the PE changed the photomicrographs of casein-based nanocarriers and the space among spherical particles slightly increased. According to the photomicrographs of casein-based nanocarriers, spherical shape decreased directly with increasing NaCas concentration (ratio of NaCas to PE), that is, tending

to flattening increased. According to the results of some researchers, particles with smooth surfaces have less contact areas than surfaces with cracking or roughness which lead to well encapsulation, a lower gas permeability and better protection of encapsulant.[29] According to the data attained in the present research, FP1, FP3, FP6, FP7 that showed the suitable stability in terms of DLS properties (particle size, PDI, zeta potential), EE and color properties were selected for further investigations.

X-ray diffraction analysis

FIGURE 2 shows XRD patterns of the selected PE-loaded/void casein-based nanocarriers (FP1, FP3, FV1, FP6, FP7, and FV2). All the treatments presented similar profiles with peaks at 21.35°, 21.62°, 21.28°, 19.47°, 19.71°, and 19.73°, in accordance with the literature.[40] The crystallinity index calculated for the different nanocarriers was significantly different. The lower value (49 and 48% for FV1 and FV2, respectively) was obtained for empty nanocarrier while an increase was observed for PE-loaded nanocarriers 68% (FP3), 59.7% (FP7), 57.7% (FP1), 51% (FP6), for PE-loaded/void nanocarriers. Probably, this behavior is owing to the PE presence that affected the crystalline structure of the nanocarriers. However, in the diffractograms of PE-loaded casein-based nanocarrier the presence of PE specified peaks was not observed. It is assumed that amount of PE is inadequate to change the peaks of diffractogram, or PE is molecularly diffused in the matrix.

DSC measurements

The DSC analysis was performed to characterize the thermal behavior of nanocarriers and the interaction between components. The thermograms are summarized in Figure 3, and the corresponding data are epitomized in Table 3. The DSC thermogram of PE displayed two endothermic peaks at about 50°C and in the range 120.5–133.1°C
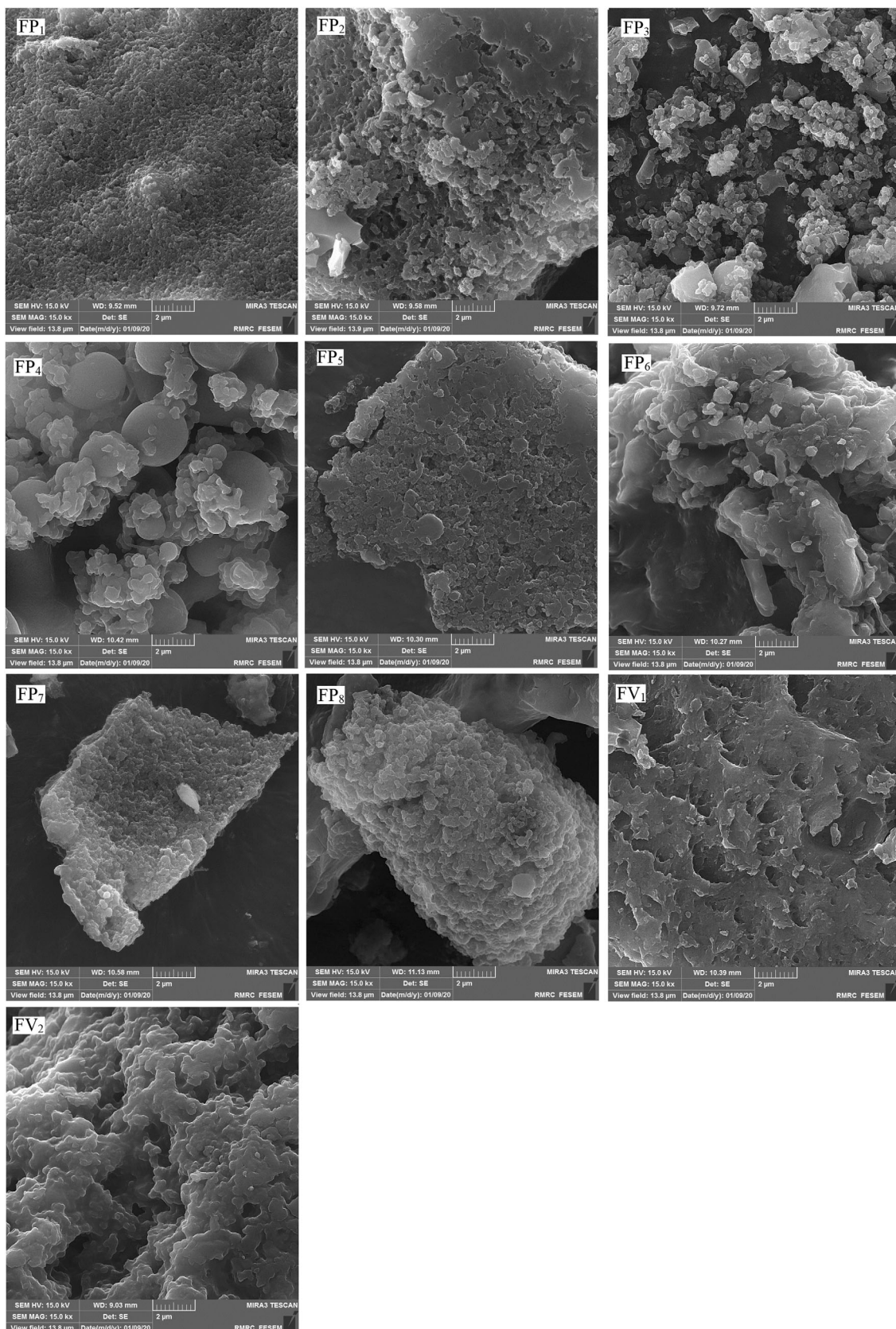
FIGURE 1 Field-emission scanning electron microscopy micrographs of propolis extract-loaded/void casein-based nanocarriers (FP1, FP2, FP3, FP4, FP5, FP6, FP7, FP8, FV1, and FV2) at the magnification of 2 μm.
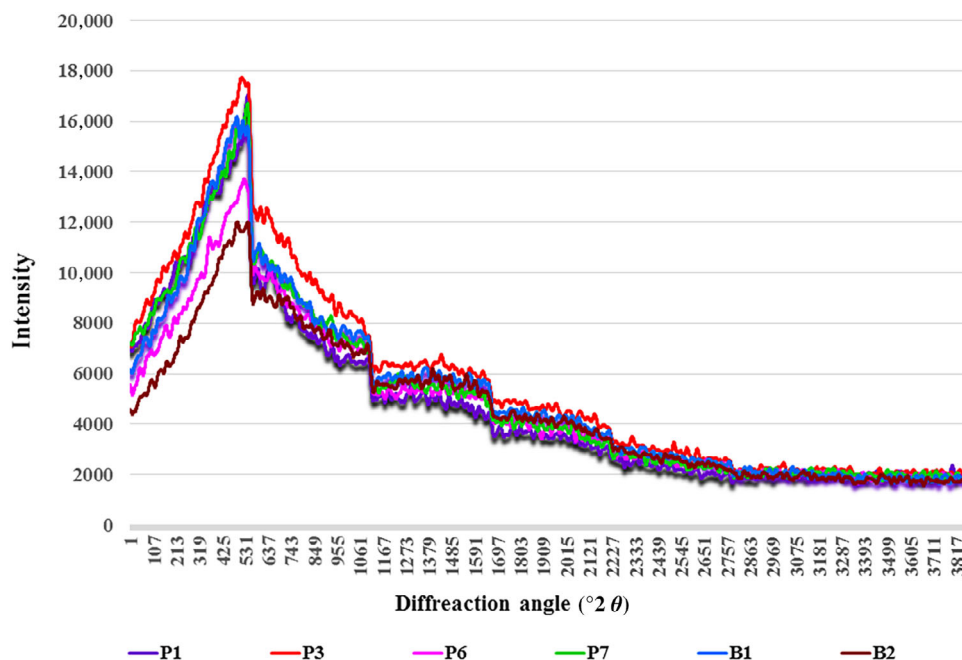
FIGURE 2   X-ray diffraction analysis of propolis extract-loaded/void casein-based nanocarriers (FP1, FP3, FP6, FP7, FV1, FV2).
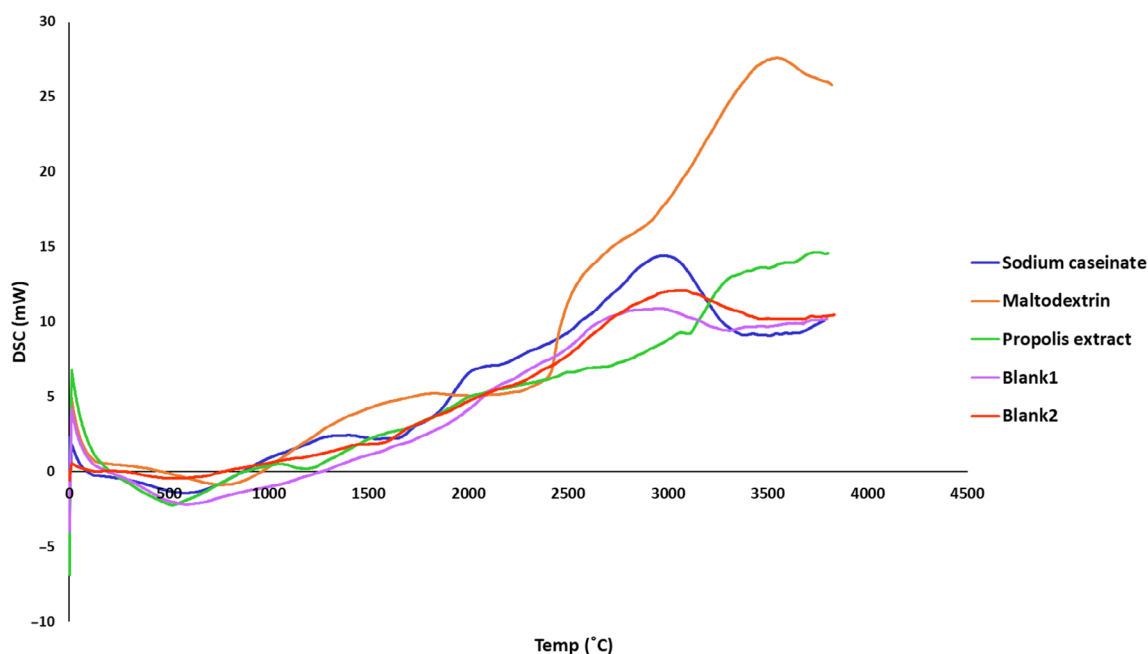
FIGURE 3   Differential scanning calorimetry curves of initial components and propolis extract and void casein-based carriers.

attributed to the PE melting. Instead, DSC curve of NaCas present an endothermic peak in the range 73–75°C, attributable to a melting phenomenon and a relatively wide exothermic peak in the range 299–318.6°C, related to a decomposition. Similar results were obtained for void nanocarriers (FV1 and FV2) while a difference was observed PE-loaded casein-based carriers. The DSC thermograms of FP3 and FP6 displayed two endothermic peaks in the range 40.9–77.8°C and 43.7–

75.2°C attributable to the PE melting and two sharp exothermic peaks in the range 329.9–324.3°C and 289–319.1°C ascribed to the NaCas thermal decomposition. Instead, the DSC thermograms FP1, FP7 displayed just the exothermic peak in the range 290.7–322.2°C and 288.8–322.1°C that corresponds to NaCas thermal decomposition. Even if PE melting peak is not evident, an increase of the slope of the thermograms probably indicate formation of hydrogen bonds with

TABLE 3 Melting temperature and enthalpy for void casein-based carriers and PE-loaded selected formulations.

Factor	NaCas	PE	FP1	FP3	FV1	FP6	FP7	FV2
Teo (°C)	299.4 ± 6.74A	120.5 ± 3.17B	290.7 ± 8.16b	40.9 ± 1.34e 323.9 ± 5.45a	271.9 ± 8.36c	43.7 ± 2.31d 289.2 ± 6.73b	288.8 ± 8.19b	282.8 ± 7.19c
Tm (°C)	318.6 ± 5.41A	133.1 ± 4.33B 50 ± 1.25C	322.2 ± 10.46b	77.8 ± 3.52e 324.3 ± 6.56a	316.0 ± 7.42e	75.2 ± 3.20f 319.1 ± 5.17c	322.1 ± 9.43b	322.9 ± 5.36b
ΔH (J/g)	41.89 ± 2.61A	7.86 ± 0.92B	52.27 ± 9.52b	40.5 ± 2.18 82.85 ± 3.12a	39.16 ± 2.15d	50.95 ± 3.15c 50.59 ± 2.44c	51.66 ± 1.65b	33.34 ± 1.39e

Note: Teo, start of melting temperature; Tm, end of melting temperature, ΔH, melting enthalpy. Different lower-case letters (among different nanocarriers) and capital letters (between initial components) indicate a significant difference at $p < 0.05$ in each row.
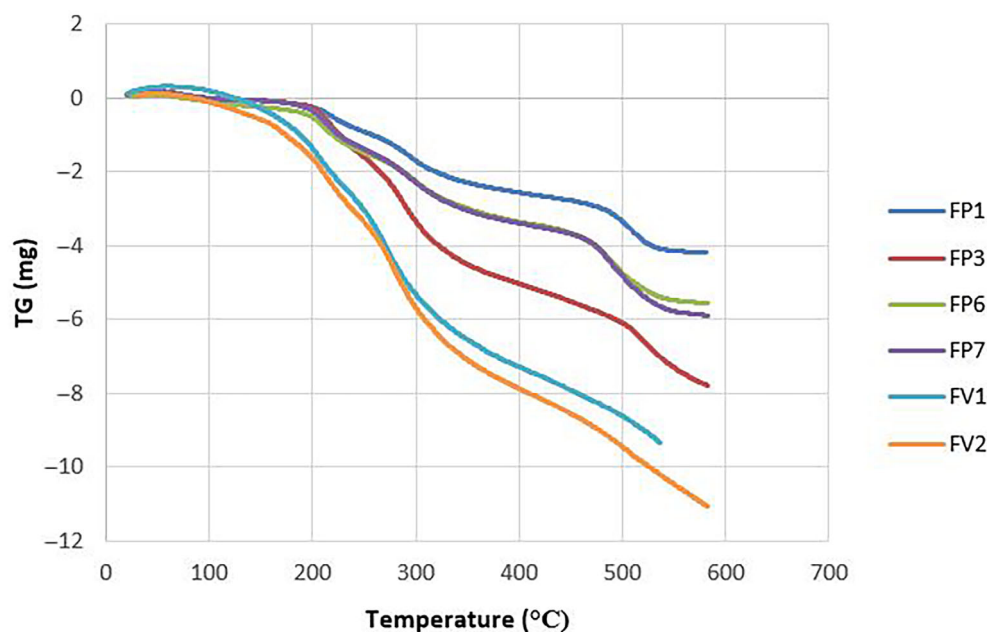
FIGURE 4 Thermogravimetric analysis thermograms of propolis extract and void casein-based carriers.

hydroxyl and ester groups in NaCas and PE as well as hydrophobic bonds and Van-der-Waals bonds among non-polar sections in colloid forms. In other research, similar results have also been recorded.[31,41] On the other hand, by comparing the DSC thermogram of PE, void casein-based carriers (FP1, FP2) and PE-loaded casein-based carriers, it was realized that width and height of the peaks increased with the higher ratios of PE applied (i.e., FP1 = 1:10 and FP3 = 1:2.5), while with the higher ratios of NaCas (i.e., FP6 = 1:10 and FP7 = 1:5), this efficacy approximately disappeared or severely decreased. These results were anticipated, whenever NaCas was at higher levels within carriers compared with PE, PE-loaded casein-based carriers were envisaged to react uniformly to pure NaCas than to pure PE. Anyway, it is probable increase in width of the peaks indicates decrease in the crystallinity or variety of crystals. Moreover, PE melting peak is not appreciable in all the nano carriers. This phenomenon is probably due to the thermal effect of the technique or to a non- crystalline encapsulation of PE in carriers.

TGA and DTA

Difference in thermograms of casein-based carriers containing PE and void casein-based carriers (FV1 and FV2) were investigated by TGA (Figure 4) while the single thermographs are reported as Supplementary Materials. According to TGA curves, it was found that a small mass loss exists in all TGA curves along with increasing temperature (100°C) which is due to sample dehydration. After a consecutive term of stable mass, a renewed mass loss was observed, at lower temperature for void protein-based carriers (FV1: 130°C and FV2 = 162°C) and at higher temperature for loaded nanocarriers (200, 204, 196, and 196°C for FP1, FP3, FP6, and FP7 respectively). The results show PE presence increases the thermal resistance probably due to the interactions between core and wall materials or the effect of phenol compounds on thermal stability. As shown in the Figure 4, the slopes of PE-loaded nanocarriers diminished leisurely with temperature compared with void nanocarriers. The higher decomposition temperature
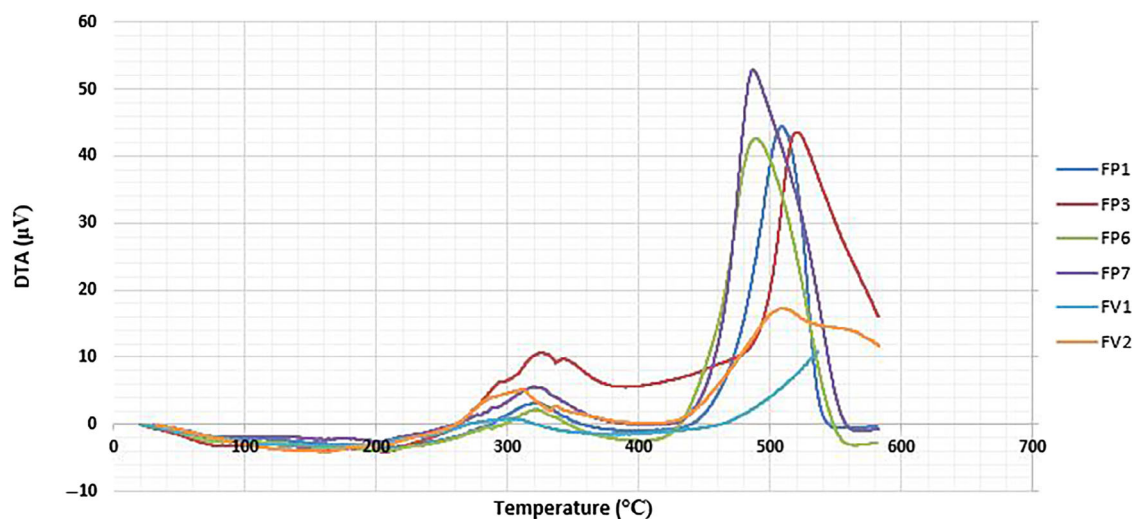
FIGURE 5 Differential thermal analysis curves of propolis extract and void casein-based carriers.

and thermal resistance was observed for higher PE content. Therefore, it can be concluded that the addition of PE led to thermal stability of protein-based carriers, thus supporting the conclusion of a positive effect of phenol compounds on thermal stability of protein nanocarrier. The DTA curves of casein-based carriers containing PE and void casein-based carriers (FV1 and FV2) are displayed in Figure 5. The casein-based carriers containing PE (FP6 and FP7) submitted a similar TGA (three stages) and DTA (two stages) curves at 196°C, 347/349°C, 581/578°C as well as 323 and 488°C, respectively. All the samples, except FP3, exhibited two stages of the thermal degradation; nevertheless, slight differences could be seen between their thermal patterns. The primary stages apperceived in the range 25.5–389.74°C, 25.3–409°C, 25°C to 418.84 as well as 25.1–421.48°C (for FP1, FP3, FP6, and FP7 respectively) may be associated with the dehydration or removal of volatile material, dissociation of –COO groups, and oxidation and depolymerization reactions of amino and carboxylic groups of wall materials (NaCas). In casein-based carriers containing propolis the second degradation depicted in the ranges of 389.83–546°C, 409.31–582°C, 419.11–582°C, and 421.72–582°C (for FP1, FP3, FP6, and FP7, respectively) may be related to the presence of PE encapsulated in casein-based carriers. A significantly higher temperature of depreciation was discerned for casein-based carriers containing PE compared with the void casein-based carriers which are ascribed to the presence of PE and stability of PE-loaded nanocarriers with high mobility of its components.[1] Overall, with the addition of PE, the thermal stability of the d casein-based carriers was ameliorated and a reduced weight loss of casein-based carriers containing PE was apperceived in DTA curves. Finally, the casein-based carriers produced exhibited outstanding values of TGA and DTA compared with previous investigations[1] and these results exhibited that propolis improve the thermal stability of casein-based nanocarriers.

CONCLUSION

In this study, PE-loaded casein-based nanocarriers was successfully fabricated aimed for the protection of PE as food supplements. As seen from results of this work, the PE-loaded casein-based nanocarriers had an appropriate particle size, stability, and a good encapsulation depending on PE:NaCas ratio and NaCas content. The results of XRD, DSC, and TGA/DTA analysis disclosed that PE was capable to be molecularly disseminated in the polymeric matrix, persuading a significantly increase on its thermal stability. Future studies will be focused on the evaluation of the long/short-term stability of the nanocarriers, anti-microbial and functional properties. To conclude, PE encapsulated within casein nanocarriers represented convenient physicochemical attributes and could provide as bioactive load in food/medical system.

CONFLICT OF INTEREST STATEMENT
The authors declare no conflicts of interest.

ORCID
Francesca Maestrelli https://orcid.org/0000-0002-7732-7381

REFERENCES
1. Nori MP, Favaro-Trindade CS, Matias de Alencar S, Thomazini M, de Camargo Balieiro JC, Contreras Castillo CJ. Microencapsulation of propolis extract by complex coacervation. LWT. 2011;44:429–35.
2. Soleimanian Y, Goli SAH, Shirvani A, Elmizadeh A, Marangoni AG. Wax-based delivery systems: preparation, characterization, and food applications. Compr Rev Food Sci Food Saf. 2020;19:2994–3030.

3. Castro ML, do Nascimento AM, Ikegaki M, Costa-Neto CM, Alencar SM, Rosalen PL. Identification of a bioactive compound isolated from Brazilian propolis type 6. Bioorg Med Chem. 2009;17:5332–5.

4. Busch VM, Pereyra-Gonzalez A, Segatin N, Santagapita PR, Poklar Ulrih N, Buera MP. Propolis encapsulation by spray drying: characterization and stability. LWT. 2017;75:227–35.

5. Cottica SM, Sabik H, Antoine C, Fortin J, Graveline N, Visentainer JV, et al. Characterization of Canadian propolis fractions obtained from two-step sequential extraction. LWT. 2015;60:609–14.

6. Elbaz NM, Khalil IA, Abd-Rabou AA, El-Sherbiny IM. Chitosan-based nano-in-microparticle carriers for enhanced oral delivery and anticancer activity of propolis. Int J Biol Macromol. 2016;92:254–69.

7. Chen H, Wooten H, Thompson L, Pan K. Nanoparticles of casein micelles for encapsulation of food ingredients. In: Jafari SM, editor. Biopolymer nanostructures for food encapsulation purposes. Volume 1. London: Academic Press; 2019. p. 39–68.

8. Powers KW, Brown SC, Krishna VB, Wasdo SC, Moudgil BM, Roberts SM. Research strategies for safety evaluation of nanomaterials: characterization of nanoscale particles for toxicological evaluation. Toxicol Sci. 2006;2:296–303.

9. Cushen M, Kerry J, Morris M, Cruz-Romero M, Cummins E. Nanotechnologies in the food industry – recent developments, risks and regulation. Trends Food Sci. 2012;24:30–46.

10. Assadpour E, Mahdi Jafari S S. A systematic review on nanoencapsulation of food bioactive ingredients and nutraceuticals by various nanocarriers. Crit Rev Food Sci Nutr. 2019;59:3129–51.

11. Jafari SM, Paximada P, Mandala I, Assadpour E, Mehrnia MA. Encapsulation by nanoemulsions. In: Jafari SM, editor. Nanoencapsulation technologies for the food and nutraceutical industries. Gorgan, Iran: Gorgan University of Agricultural Sciences and Natural Resources; 2017. p. 36–73.

12. Penalva R, Esparza I, Agüeros M, Gonzalez-Navarro CJ, Gonzalez-Ferrero C, Irache JM. Casein nanoparticles as carriers for the oral delivery of folic acid. Food Hydrocoll. 2015;44:399–406.

13. Moeiniafshari AA, Zarrabi A, Bordbar AK. Exploring the interaction of naringenin with bovine beta-casein nanoparticles using spectroscopy. Food Hydrocoll. 2015;51:1–6.

14. Dima C, Assadpour E, Dima S, Jafari SM. Bioactive-loaded nanocarriers for functional foods: from designing to bioavailability. Curr Opin Food Sci. 2020;33:21–9.

15. Beikzadeh S, Khezerlou A, Jafari SM, Pilevar Z, Mortazavian AM. Seed mucilages as the functional ingredients for biodegradable films and edible coatings in the food industry. Adv Colloid Interface Sci. 2020;280:102164.

16. Bylund G. Dairy processing handbook. 1st ed. Lund: Tetra Pak Processing Systems AB; 2015.

17. Shendurse A. Milk protein based edible films and coatings–preparation, properties and food applications. JNHFE. 2018;8:2.

18. Khwaldia K, Perez C, Banon S, Desobry S, Hardy J. Milk proteins for edible films and coatings. Crit Rev Food Sci Nutr. 2004;44:239–51.

19. Forrest SA, Yada RY, Rousseau D. Interactions of vitamin D 3 with bovine β-lactoglobulin A and β-casein. J Agric Food Chem. 2005;53:8003–9.

20. Zimet P, Rosenberg D, Livney YD. Re-assembled casein micelles and casein nanoparticles as nano-vehicles for ω-3 polyunsaturated fatty acids. Food Hydrocoll. 2011;25:1270–6.

21. Shapira A, Davidson I, Avni N, Assaraf YG, Livney YD. β-Casein nanoparticle-based oral drug delivery system for potential treatment of gastric carcinoma: stability, target-activated release and cytotoxicity. Eur J Pharm Biopharm. 2012;80:298–305.

22. Wijayanto A, Putri YRP, Hermansyah H, Sahlan M. Encapsulation of eugenol from clove oil using casein micelle for solid preparation. Depok City: AIP Publishing; 2017. 030012. https://doi.org/10.1063/1.4976781

23. Santos Basurto MA, Cardador Martínez A, Castaño Tostado E, Bah M, Reynoso Camacho R, Amaya Llano SL. Study of the interactions occurring during the encapsulation of sesamol within casein micelles reformed from sodium caseinate solutions: study of casein-sesamol interactions. J Food Sci. 2018;83:2295–304.

24. Ghayour N, Hashem Hosseini SM, Eskandari MH, Esteghlal S. Nanoencapsulation of quercetin and curcumin in casein-based delivery systems. Food Hydrocoll. 2019;87:394–403.

25. Liu Q, Han C, Tian Y, Liu T. Fabrication of curcumin-loaded zein nanoparticles stabilized by sodium caseinate/sodium alginate: curcumin solubility, thermal properties, rheology, and stability. Process Biochem. 2020;94:30–8.

26. Nogueira MH, Tavares G, Casanova F. Cross-linked casein micelle used as encapsulating agent for jaboticaba (*Plinia jaboticaba*) phenolic compounds by spray drying. Int J Dairy Technol. 2020;73:765–70.

27. Soleimanifard M, Feizy J, Maestrelli F. Nanoencapsulation of propolis extract by sodium caseinate-maltodextrin complexes. Food Bioprod Process. 2021;128:177–85.

28. Silva JC, Rodrigues S, Feás X, Estevinho LM. Antimicrobial activity, phenolic profile and role in the inflammation of propolis. Food Chem Toxicol. 2012;50:1790–5.

29. da Silva FC, Rodrigues da Fonseca C, Matias de Alencar S, Thomazini M, de Carvalho Balieiro S, Pittia P, et al. Assessment of production efficiency, physicochemical properties and storage stability of spray-dried propolis, a natural food additive, using gum Arabic and OSA starch-based carrier systems. Food Bioprod Process. 2013; 91:28–36.

30. Umesha SS, Monahar B, Naidu KA. Microencapsulation of α-linolenic acid-rich garden cress seed oil: physical characteristics and oxidative stability. Eur J Lipid Sci Technol. 2013;115:1474–82.

31. Osojnik Crnives IG, Istenic K, Ota A, Megusar P, Slukan A, Humar M, et al. Encapsulation of non-dewaxed propolis by freeze-drying and spray-drying using gum Arabic, maltodextrin and inulin as coating materials. Food Bioprod Process. 2019;116:196–211.

32. Andrade JKS, Denadai M, de Oliveira CS, Nunes ML, Narain N. Evaluation of bioactive compounds potential and antioxidant activity of brown, green and red propolis from Brazilian northeast region. Food Res Int. 2017;101:129–38.

33. Kazemi F, Divsalar A, Saboury AA, Seyedarabi A. Propolis nanoparticles prevent structural changes in human hemoglobin during glycation and fructation. Colloids Surf B Biointerfaces. 2019;177:188–95.

34. Soleimanian Y, Goli SAH, Varshosaz J, Maestrelli F. Propolis wax nanostructured lipid carrier for delivery of β sitosterol: effect of formulation variables on physicochemical properties. Food Chem. 2018; 260:97–105.

35. Moser P, Telis VRN, de Andrade NN, García-Romero E, Gómez-Alonso S, Hermosín-Gutiérrez I. Storage stability of phenolic compounds in powdered BRS Violeta grape juice microencapsulated with protein and maltodextrin blends. Food Chem. 2017;214:308–18.

36. Lee HS. Objective measurement of red grapefruit juice color. J Agric Food Chem. 2000;48:1507–11.

37. Maskan M. Production of pomegranate (*Punica granatum* L.) juice concentrate by various heating methods: colour degradation and kinetics. J Food Eng. 2006;72:218–24.

38. Obón JM, Castellar MR, Alacid M, Fernández-López JA. Production of a red–purple food colorant from *Opuntia stricta* fruits by spray drying and its application in food model systems. J Food Eng. 2009; 90:471–9.

39. Mahdavee Khazaei K, Jafari SM, Ghorbani M, Hemmati Kakhki A. Application of maltodextrin and gum Arabic in microencapsulation of saffron petal's anthocyanins and evaluating their storage stability and color. Carbohydr Polym. 2014;105:57–62.

40. Sica de Toledo LA, Belloto de Francisco LM, Esposito E, Lim Y, Valacchi G, Luciano Bruschi M. Nanostructured lipid systems

modified with waste material of propolis for wound healing: design, in vitro and in vivo evaluation. Colloids Surf. 2017;B158:441–52.

41. Narasagoudr SS, Hegde VG, Vanjeri VN, Chougale RB, Masti SP. Ethyl vanillin incorporated chitosan/poly (vinyl alcohol) active films for food packaging applications. Carbohydr Polym. 2020;236:116049.

SUPPORTING INFORMATION

Additional supporting information can be found online in the Supporting Information section at the end of this article.